Planar Printed Wideband Filtering Quasi-Yagi Antenna and Its Notch-Band Design Using Parasitic Elements for Vehicular Communication

Daotong Li, *Senior Member, IEEE*, Chen Yang, Ying Liu, Lisheng Yang, and Qiang Chen, *Senior Member, IEEE*

***Abstract*—A compact planar printed wideband filtering quasi-Yagi antenna without any extra external filtering circuit for vehicular communication is proposed in this article. It consists of a microstrip-to-slotline transition (MST), a coplanar stripline (CPS), driven elements and parasitic elements which act as directors and filtering elements simultaneously. The MST can inherently introduce four radiation nulls on the lower and upper stopband, and by adding a pair of exponential curved branch elements symmetrically, two radiation nulls are generated on the upper stopband. Moreover, four parasitic elements are placed around the director to enhance the end-fire radiation and the rejection levels of three radiation nulls on the upper stopband. Therefore, a wideband filtering quasi-Yagi antenna with a good endfire characteristics with the measured bandwidth of 4.46 to 11.31 GHz (∼86.9%), a peak gain of 8.3 dBi, and the out-of-band suppression larger than 14 dB is achieved, without any additional external filtering circuits. When a pair of L-shaped parasitic elements are symmetrically placed on the top layer, a notch with −20.5 dBi measured gain rejection in the working frequency band can be introduced, which guarantees good interference suppression ability. The measured results show good agreement with the simulation. The proposed antennas are good candidates for in-vehicle Wi-Fi 6E, in-vehicle satellite communication, mobile-service, V2V communication applications.**

***Index Terms*—Vehicular communication, quasi-Yagi antenna, endfire, filtering antenna, notched-band, wideband, parasitic elements.**

Manuscript received 24 March 2023; revised 6 July 2023 and 3 September 2023; accepted 7 September 2023. Date of publication 13 September 2023; date of current version 13 February 2024. This work was supported in part by the National Natural Science Foundation of China under Grant 61801059, in part by the FY2021 Japan Society for the Promotion of Science (JSPS) Postdoctoral Fellowship for Research in Japan under Grant P21053, and in part by the Grant-in-Aid for JSPS Research Fellow under Grant 21F21053, in part by the Opening Fund of State Key Laboratory of Mm-Waves under Grant K202016, and in part by the Basic Research and Frontier Exploration Special of Chongqing Natural Science Foundation under Grant cstc2019jcyj-msxmX0350. The review of this article was coordinated by Prof. Han Lim Lee. *(Corresponding authors: Daotong Li; Ying Liu.)*

Daotong Li is with Center of Aerocraft TT&C and Communication and School of Microelectronics and Communication Engineering, Chongqing University, Chongqing 400044, China, and also with the Department of Communications Engineering, Tohoku University, Sendai 980-8579, Japan (e-mail: dli@cqu.edu.cn).

Chen Yang, Ying Liu, and Lisheng Yang are with the School of Microelectronics and Communication Engineering, Chongqing University, Chongqing 400044, China (e-mail: 1878832065@qq.com; liuyingcqu@cqu.edu.cn; yls@cqu.edu.cn).

Qiang Chen is with the Department of Communications Engineering, Tohoku University, Sendai 980-8579, Japan (e-mail: qiang.chen.a5@tohoku.ac.jp).

Digital Object Identifier 10.1109/TVT.2023.3314974

I. Introduction

With the rapid development of 5G MIMO and vehicular communications, the space of vehicles is getting smaller and the equipment is getting more integrated. To accommodate the limited space of vehicle environment, compact, wideband and low-profile antennas are widely used [1], [2], [3]. Furthermore, the electromagnetic environment of the vehicles is more complicated because of the growing number of radio frequency devices. To guarantee the communication quality of vehicles, out-of-band interference should be suppressed by some means. With the excellent suppression capability and compact structure, filtering antennas are good candidate for the application of vehicular system in limited space [4]. In addition, as the increasing applications in different bands, as shown in Fig. 1, such as 5G for vehicle-to-everything communication (V2X), 5.2-GHz WLAN, satellites communication (5.85–6.425 GHz, 8/7 GHz), and mobile-service (10–10.5 GHz), and thus the broadband antenna covering several frequency bands is a good solution for reducing the number of antennas in limited space [5], [6]. Hence, compact wideband filtering antennas for vehicular communication are urgently desired.

Compared with filtering patch antenna [7], [8], filtering monopole antenna [9], [10] and filtering dielectric antenna [11], [12] reported recently, the filtering quasi-Yagi antenna has the advantages of good endfire radiation pattern and wideband characteristics [13], [14], [15]. In the traditional design process, the design methods of filtering quasi-Yagi antenna can be divided into following three categories. Firstly, filter synthesis design methods are applied by integrating the antenna radiator as the last-stage resonator of the filter [16], [17]. However, large insertion loss and the occupied size of filtering antennas are unavoidable. Cascading the antenna and filter units is another method. In [18], although the filtering function is implemented by integrating filter unit in slotline which makes the structure complex, and the bandwidth is narrow, as well. In [19], five radiation nulls are created by integrating a bandstop unit. However, the gain is low though it has good suppression ability. To avoid the drawback, the design method of filtering antennas with embedded filter unit into the feed line or the reflector are proposed. Nonetheless, structure and design complexities are increased, and huge fine-tuning works are required [20], [21], [22]. Through using offset double-sided parallel-strip line, the

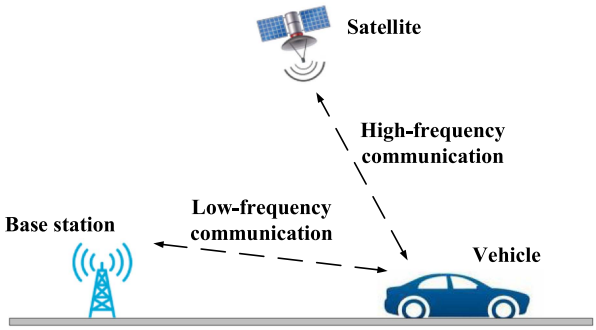

Fig. 1. Application in different bands of vehicles.

performance of filtering and low profile has been acquired in [20], but the bandwidth needs to be improved. Filtering ability and flat gain are obtained by adding absorptive-branch-load in [21], while the out-of-band suppression is limited. In [22], by replacing the dipole and director with dielectric resonator and near-zero-index metamaterial, the high gain filtering antenna is realized, but the large size and high profile are also achieved due to the dielectric resonator unit. Thus, a compact wideband filtering planar Yagi antenna is quite desired.

Moreover, due to the fact that there usually exist interferences in the working frequency band of a wideband antenna. To guarantee the reliability of the vehicular communication system, setting the notched bands in the typical frequency band has become one of the prevailing solutions to suppress the interferences [23].

To realize the band-notched characteristics, researchers have developed many design methods [24], [25], [26]. In [24], by using two orthogonal crossed dipoles and two Y-shaped baluns, a notched band for 2.9–3.2 GHz is realized. However, its profile is high due to the 3D structure. In [25], a notched band from 4.9 to 6.6 GHz is obtained by the open/short circuited resonator located on the slot of the traditional Vivaldi antenna. In [26], by using meander shaped DGS slots, four notched bands are realized.

In this article, a compact planar printed wideband filtering quasi-Yagi antenna without external filtering circuit is proposed. Six radiation nulls (RN), RN_1, RN_2 on the lower stopband and RN_3, RN_4, RN_5 and RN_6 on the upper stopband, are introduced to improve the passband selectivity and out-of-band suppressions. Through the microstrip-to-slot transition (MST) and coplanar stripline (CPS), four inherit radiation nulls RN_1, RN_2, RN_3 and RN_4 are generated, and RN_5 and RN_6 are generated by the pair of symmetrical exponential curved branch elements located at the connection point of slotline and CPS. Moreover, the rejection levels of RN_3, RN_4 and RN_5 are further improved by adding two pairs of parasitic elements around the director. A prototype of filtering antenna with broadband of 4.46 to 11.31 GHz is achieved, which can realize 5.5-GHz WLAN, in-vehicle Wi-Fi 6E (5.925–7.125 GHz), in-vehicle satellite communication (5.85–6.425 GHz, 8/7 GHz), and mobile-service (10–10.5GHz). In order to introduce the notch band to reject the in-band interferences, by adding a pair of parasitic elements with step impedance resonator (SIR) characteristics on the top layer,

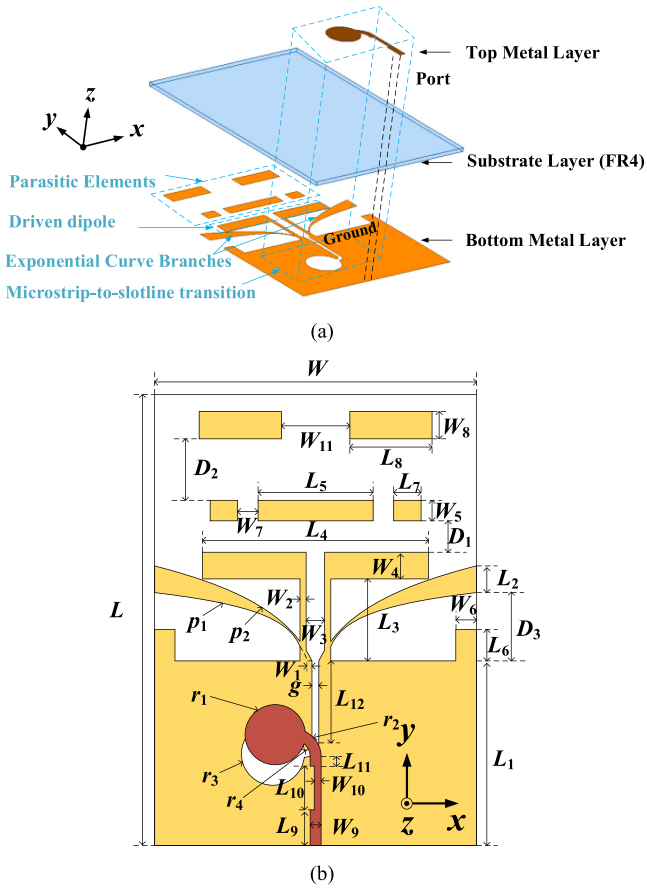

Fig. 2. Proposed structure of wideband filtering quasi-Yagi antenna, (a) 3D view, (b) configuration and its parameters.

an integrated filtering quasi-Yagi antenna with an in-band notch is further realized with the whole performance almost no change, and the radiation null depth is −25 dBi at 7.34 GHz, whose frequency band can be adjusted to suppress possible in-band interferences in practice. To the best of the authors' knowledge, there is no filtering quasi-Yagi antenna with notch characteristics reported.

The arrangement of this article is as follows. Section II is the working mechanism analysis, design process and measurement of the proposed compact wideband filtering quasi-Yagi antenna. Section III gives the working principle of the notch, the parameters analysis and the measurement of the filtering quasi-Yagi antenna with band-notched characteristics. Finally, conclusion is drawn in Section IV.

II. Design and Analysis of Wideband Filtering Quasi-Yagi Antenna

Based on the integration design method, a compact planar printed wideband quasi-Yagi filtering antenna without external filtering circuit is proposed, which is shown in Fig. 2, and its configuration, operating mechanism and numerical analysis are detailed as follows.

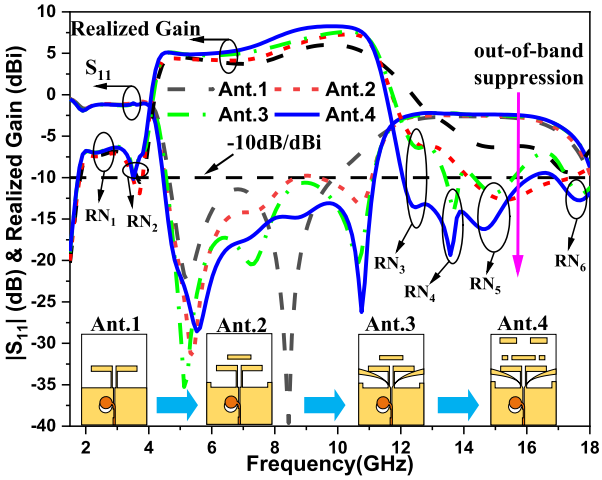

Fig. 3. Evolution of the proposed antenna and their performances.

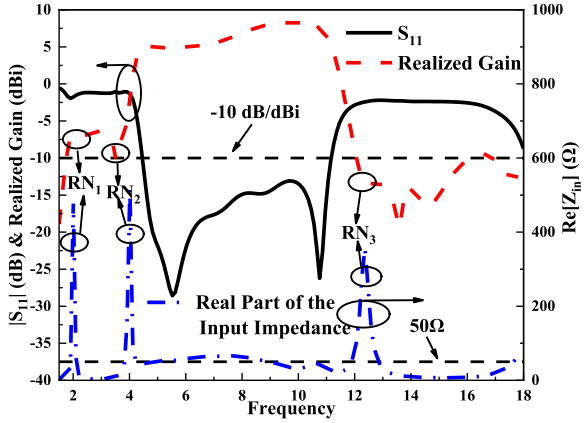

Fig. 4. Reflection coefficient, realized gain of the proposed antenna and real part of input impedance.

A. Antenna Configuration

Fig. 2(a) shows the configuration of the proposed planar printed wideband filtering quasi-Yagi antenna, which just one layer of FR4 dielectric substrate with a permittivity of 4.4, loss tangent tanδ of 0.02 and a thickness of 0.5mm is used. It is composed of three layers in total, including two metal layers, named top and bottom metal layers, respectively, and one dielectric layer named as substrate layer (FR4). The feeding structure contains the feedline and MST consisting of a microstrip circular stub loaded at the end of the microstrip line on the top metal layer and a slot circular stub located at one end of the slotline on the bottom metal layer, respectively. On the bottom metal layer, the dipole is connected to the MST through the CPS. Additionally, two rectangular stubs are placed at the edge of the reflector to enlarge the equivalent length of the reflector. Furthermore, a pair of exponential curved branch elements are set from the slotline to the edge of the substrate to introduce radiation nulls. Finally, a director with four parasitic elements is placed upon the dipole to improve the directivity and out-of-band suppressions. The whole size of the FR4 substrate is 33 mm $\times$ 23.5 mm (0.49 $\times$ 0.35, where is the free-space wavelength at the lowest cut-off frequency). Without using any external filtering circuits, a wideband filtering quasi-Yagi antenna is achieved, and the detailed parameters of the structure are shown in Fig. 2(b).

B. Mechanism of the Antenna

In order to gain insight into the antenna design mechanism deeply, based on the basic reference Ant.1 composed of a dipole, a reflector and MST feeding structure, the evolution of the proposed wideband filtering quasi-Yagi antenna is depicted in the inset of Fig. 3. It can be observed that the working frequency band of Ant. 1 ranges from 4.64 to 9.90 GHz with a fractional bandwidth (FBW) of 72.4% under the condition of impedance bandwidth below -10 dB. Two radiation nulls are generated in the lower stopband at 2.4 (RN_1) and 3.5 GHz (RN_2), respectively. While the radiation nulls located at 15 (RN_3) and 17 GHz (RN_4) on the upper stopband are far away from the passband, so that the roll-off rate is very limited.

Moreover, to enhance the bandwidth and the directivity of the proposed filtering quasi-Yagi antenna, a director is placed on the dipole, and the equivalent length of the reflector is enlarged by adding two extended stubs on edge of the substrate. It can be seen from the Fig. 3 that there is an additional resonance at 10.76 GHz generated by the director, which can broaden the bandwidth. It is noteworthy that the RN_3 GHz shifts to 12.77 GHz and RN_4 shifts to 15.38GHz, which improves the roll-off rate of the upper stopband. Moreover, the peak gain in the endfire direction ($+y$ axis) is also improved from 6 to 7.28 dBi.

Furthermore, for further enhancing the passband roll-off rate of the proposed filtering quasi-Yagi antenna, a pair of exponential curved branch elements are placed at the connection point of slotline and the CPS, named as Ant. 3, as shown in the inset of Fig. 3. It can be observed that two new radiation nulls (RN_5 and RN_6) on the upper band at 15 and 17.69 GHz with the depth of -11.8 and -12 dBi are introduced to further improve the selectivity. Finally, by adding two pairs of parasitic elements around the director in Ant. 4, an additional resonance is generated at 7.14 GHz. It is worth mentioning that the parasitic elements can improve the depth of the three radiation nulls, RN_3 from -6.4 to -13.6 dBi, RN_4 from -14.2 to -19.5 dBi, RN_5 from -11.8 to -16.2 dBi, and RN_6 from 12 dBi to 12.7 dBi, respectively, on the upper stopband, and maintain a wide stopband.

Thus, benefiting from the four resonant modes, the filtering quasi-Yagi antenna with -10dB impedance bandwidth of 85.1%, ranging from 4.46 to 11.17 GHz, the peak gain of 8.26 dBi, and out-of-band suppression level (the maximum gain of the passband minus the maximum gain of the stopband) of 14.5 dB can be achieved.

C. Analysis of Radiation Nulls

As described in Fig. 3, the proposed compact planar printed wideband filtering quasi-Yagi antenna possesses six radiation nulls, which improve the passband selectivity and stopband rejection greatly. Thus, it is important to further investigate the operating mechanism of these radiation nulls.

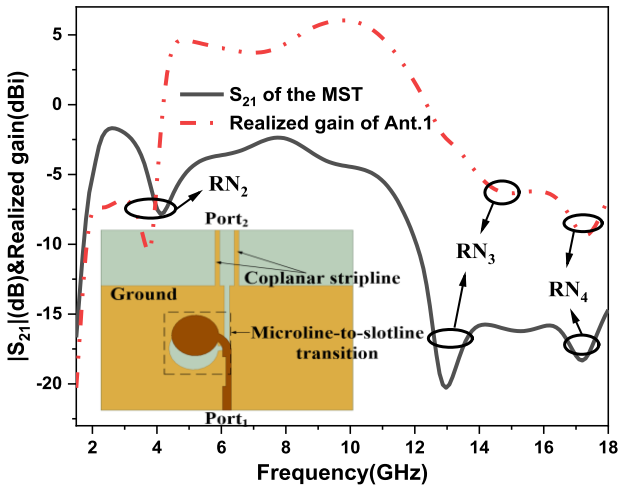

Fig. 5. S_{21} of the component and the realized gain of Ant. 1.

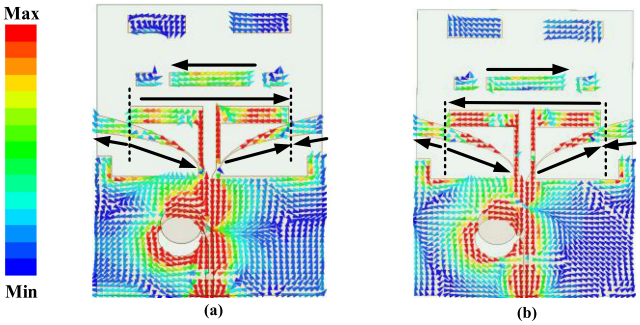

Fig. 6. Current distributions of the radiation nulls (a)RN_5 and (b)RN_6, respectively.

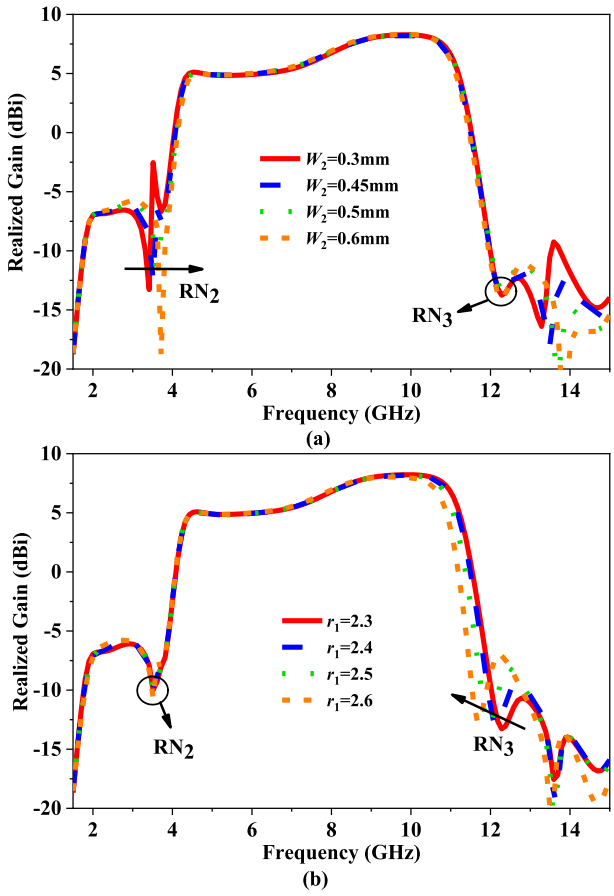

Fig. 7. Effect of the parameters (a)W_2, and (b)r_1 on the radiation nulls.

Fig. 4 shows the real part of the impendence, the S_{11} and the realized gain at the endfire direction of the proposed antenna. It can be seen that the real part of the impendence is mismatch with 50Ω severely at the frequencies of RN_1, RN_2 and RN_3. To better demonstrate the generating mechanism these radiation nulls, EM simulation and numerical analysis on the proposed microstrip-to-CPS transition (MCPST) are carried out, as shown in Fig. 5. It can be seen from the Fig. 5 that the frequencies of the radiation nulls of Ant. 1 exactly correspond to the transmission coefficient of this MCPST. Therefore, the radiation nulls are introduced inherently with the MCPST, which realizes the combination design of the filter and the wideband quasi-Yagi antenna. Thus, four radiation nulls always exist in the process of the antenna design to achieve good out-of-band suppression characteristics on both the lower and upper stopbands.

In Ant. 3, RN_5 and RN_6 are generated when a pair of exponential curved branch elements are placed at the connection point of slotline and CPS. To better clarify the mechanism of radiation RN_5 and RN_6, Fig. 6 shows the current distributions of the proposed compact planar printed wideband quasi-Yagi filtering antenna at the frequencies of radiation RN_5 and RN_6. As shown in Fig. 6(a), the vector current directions on director and exponential curved branch elements are the same, and opposite with it on the dipole. Because they have approximately equal amplitude and out of phase, the radiations on these two parts are canceled in the end-fire direction, and RN_5 is thus generated. Similarly, RN_6 is generated based on the same working principle, and Fig. 6(b) shows the current distribution at RN_6 to verify this concept.

Fig. 7(a) and (b) show the effects of W_2 and r_1 on the RN_2 and RN_3, respectively. It can be seen that as the increases of W_2, RN_2 shift to higher frequency, and when r_1 become larger, RN_3 moves towards lower frequency. Therefore, the radiation nulls of proposed filtering antenna can be controlled independently.

In order to validate the feasibility of the designs, the prototype of proposed compact wideband filtering quasi-Yagi antenna is designed, fabricated and measured. The final parameters of the proposed compact wideband filtering quasi-Yagi antenna are as follows: $L = 33$, $W = 23.5$, $L_1 = 13.5$, $L_2 = 1.95$, $L_3 = 6$, $L_4 = 16.5$, $L_5 = 8.4$, $L_6 = 2.3$, $L_7 = 2$, $L_8 = 6$, $L_9 = 2.6$, $L_{10} = 3.2$, $L_{11} = 0.7$, $W_1 = 0.55$, $W_2 = 0.45$, $W_3 = 1.35$, $W_4 = 1.95$, $W_5 = 1.5$, $W_6 = 1.5$, $W_7 = 1.5$, $W_8 = 2$, $W_9 = 0.8$, $W_{10} = 0.5$, $r_1 = 2.2$, $r_2 = 1.6$, $r_3 = 2.3$ $r_4 = 0.8$, $D_1 = 2.3$, $D_2 = 4.5$, $D_3 = 5$ $g = 0.5$ (Unit: mm).

The photograph of the proposed compact filtering quasi-Yagi antenna is shown in Fig. 8. The measured and simulated results are plotted in Fig. 9. As given in Fig. 9, the measured results show that the reflection coefficient S_{11} is less than -10 dB from 4.46 to 11.31 GHz, and the bandwidth is 86.9% which

TABLE I
COMPARISON OF THE PROPOSED ANTENNA WITH SOME EXISTING WORKS

Ref.	Design Method	FBW (%)	P. G. (dBi)	Nulls	Suppression (dB)	Extra filter	Size (λ_0^2)	Complexity
[18]	Yagi + SLR filter	18.5	5.8	2	15	Yes	0.76×0.44	Complex
[19]	Yagi + BSF	34.1	4.6	5	11	Yes	0.67×0.43	Complex
[20]	Yagi + Balanced DSPSL	30.4	5.4	2	11	Yes	0.46×0.32	Simple
[21]	Yagi + BSF	21.2	4.7	2	9	No	1.3×0.65	Complex
[22]	Yagi + DR	16.2	8.5	3	10	No	0.99×0.85	Simple
[27]	Slot + Parasitic elements + Microstrip antenna	41.9	7.3	2	15	No	0.36×0.18	Complex
This work	Yagi + Parasitic elements	85.1	8.3	6	14.5	No	0.49×0.35	Simple

Refs.: References, P.G.: Peak Gain

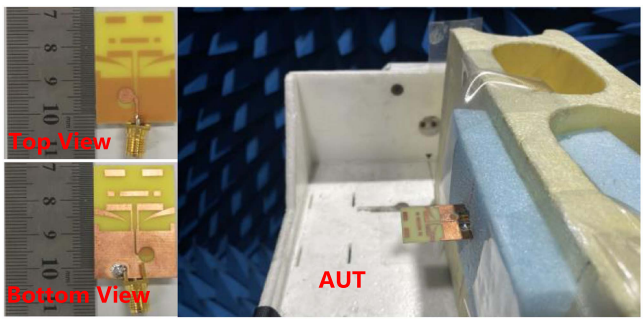

Fig. 8. Photograph of fabricated wideband quasi-Yagi filtering antenna.

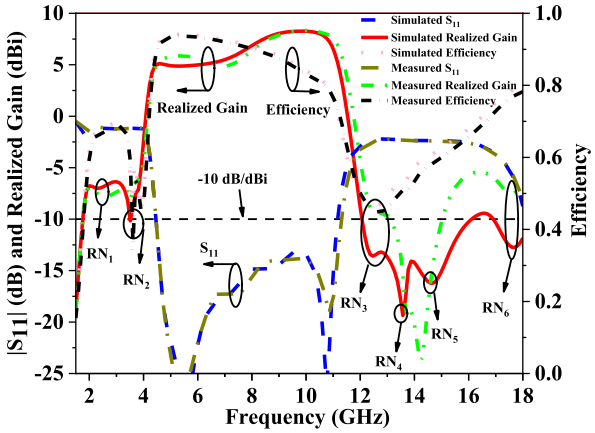

Fig. 9. Measured and simulated results of the proposed wideband filtering quasi-Yagi antenna.

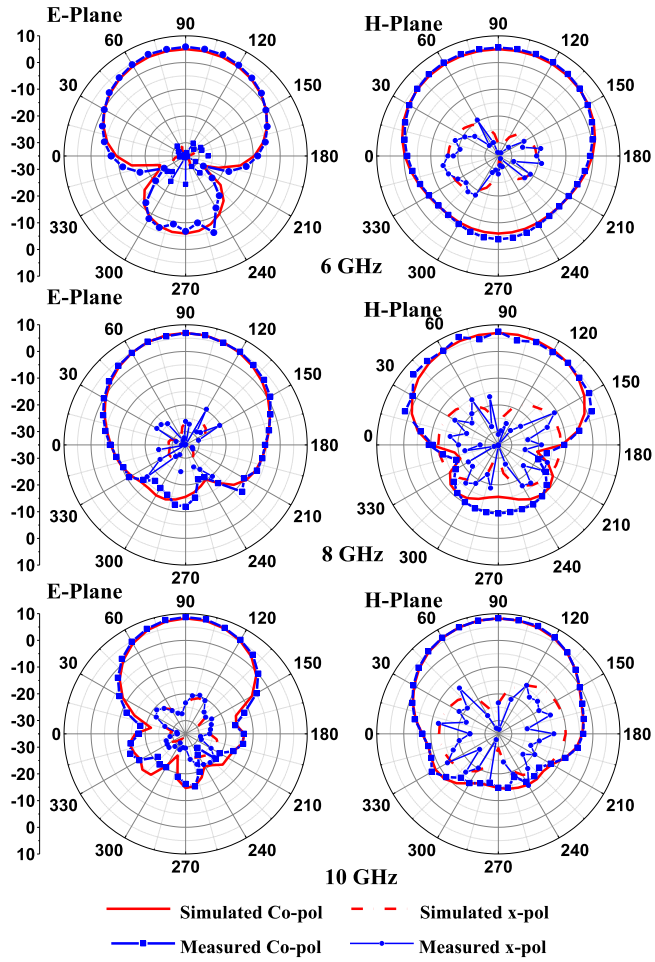

Fig. 10. Radiation patterns at (a) 6, (b) 8, and (c) 10 GHz.

is similar with the simulated one. Additionally, in the passband, the maximum gain is at 9.95 GHz with the value of 8.33 dBi, and high efficiency larger than 90% in the lower frequency and 70% in the higher frequency is obtained. Moreover, the out-of-band suppression level of the proposed antenna gain is 14 dB. Fig. 10 is the radiation patterns of the proposed antenna at 6, 8, and 10 GHz, respectively. It can be seen that the proposed antenna has good endfire characteristics in the passband. The measured cross-polarization levels are less than −20 dB and −10 dB in the E-plane and H-plane across the whole passband, respectively, and low cross-polarizations are achieved.

In order to further illustrate the advantages of the proposed antenna, in Table I, we compare the performance between the proposed antenna and other reported antennas in same type in terms of bandwidth, gain, out-of-band suppression, etc. It is obvious that the proposed antenna has the advantages of wideband, high gain and good out-of-band suppression. Additionally, there is no extra filtering circuit in the proposed antenna, and it is designed based on the substrate of FR4 and PCB processing, which is simple and low-cost.

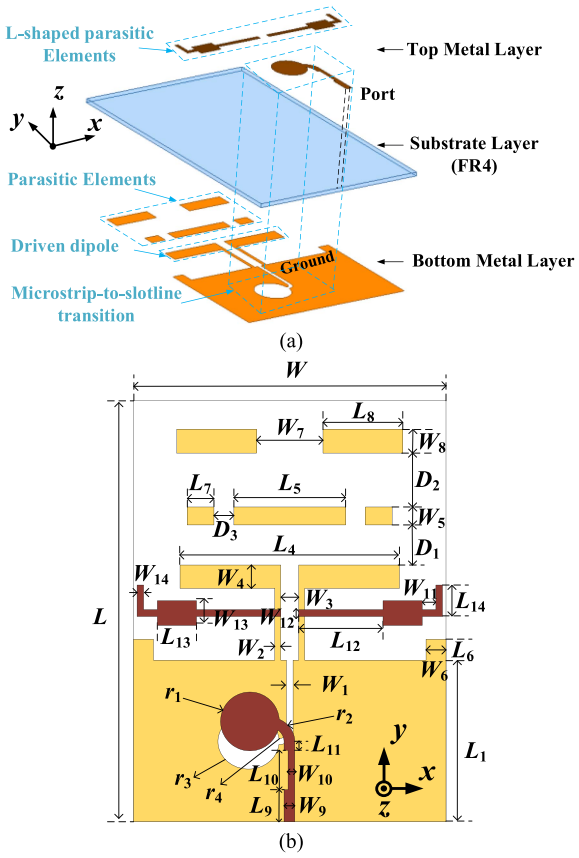

Fig. 11. Proposed wideband quasi-Yagi filtering antenna with notched-band, (a) 3D view, (b) configuration and its parameters.

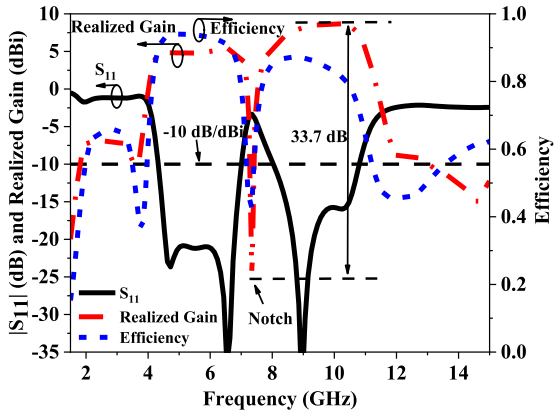

Fig. 12. Simulated results of the notched-band antenna.

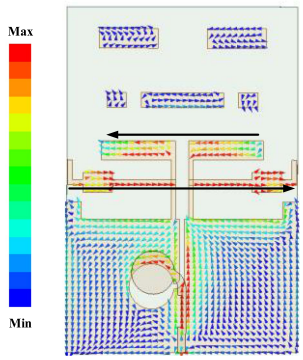

Fig. 13. Current distribution of the proposed antenna at 7.34GHz.

III. Filtering Antenna With Band-Notched Characteristics

To meet the requirement of in-band interferences suppression, the antenna with notched bands in the typical frequency band is one of the prevailing solutions. For introducing a notched-band to suppress the interference in the passband, novel parasitic elements are added on the top metal layer, as shown in Fig. 11.

A. Antenna Configuration

Fig. 11(a) shows the configuration of the proposed compact wideband filtering quasi-Yagi antenna with notched-band, and the substrate is also FR4, as well. Compared with the compact wideband filtering quasi-Yagi antenna shown in Fig. 2, the pair of exponential curved branch elements on the bottom layer is replaced by the pair of L-shaped parasitic elements with SIR characteristics on the top layer. The detailed parameters of the structure are shown in Fig. 11(b).

B. Mechanism of the Notched-band

Except for the notch band, the working mechanism of the proposed wideband filtering quasi-Yagi antenna with notched-band characteristics is similar as the wideband filtering quasi-Yagi antenna mentioned in Section II, and the simulated results are illustrated in Fig. 12. From Fig. 12, it can be obtained that the operating passband of the proposed compact wideband filtering quasi-Yagi antenna with notch band of 7.34 GHz is from 4.33 to 10.81 GHz. The peak gain in the passband is 8.7 dBi, and the depth of the notch band is −25 dBi at 7.34 GHz, which means the in-band interference suppression ability is excellent with 33.7 dB. Moreover, the out-of-band suppression in the lower and upper stopband have almost no changes compared with the wideband filtering quasi-Yagi antenna in Section II.

To reveal the mechanism of the notched-band, Fig. 13 shows the current distribution at the frequency of the radiation null of 7.34 GHz. It can be seen from Fig. 13 that the current distributions on the L-shaped parasitic elements are out of phase with that on the dipole, which means that the radiation of the dipole and the L-shaped parasitic elements are canceled. Therefore, the endfire characteristics cannot be maintained, and a notch band is thus generated.

Moreover, the frequency of the notch can be adjusted by changing the parameters of the L-shaped parasitic elements, which can be seen as an open-circuited stepped impedance resonator (SIR). Therefore, the resonant frequency of the elements can be adjusted by simply controlling the ratios of the impedance or the electrical length of the SIR. For example, it can be seen from Fig. 14, as the L_{14} increases from 1 to 3 mm, the null of the notch band is shifted from 7.17 to 7.53 GHz. Although the depth of the null decreases with the change of L_{14}, the suppression level of the notch can still achieve at least 18.7 dB, and the efficiency can maintain less than 50% at the notch. Fig. 15 shows the impact of the variation of W_{11} on the notch band, and it indicates that the larger the value of W_{11}, the higher the notch frequency band.

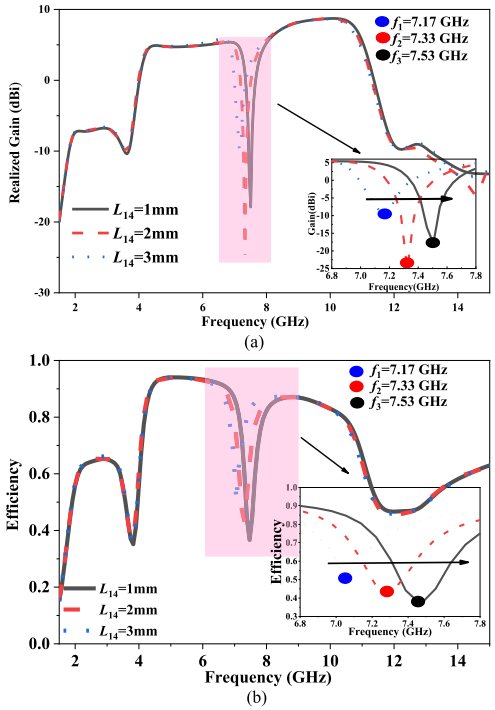

Fig. 14. Effect of the parameter L_{14} on the notched band, (a) Realized gain, (b) Efficiency.

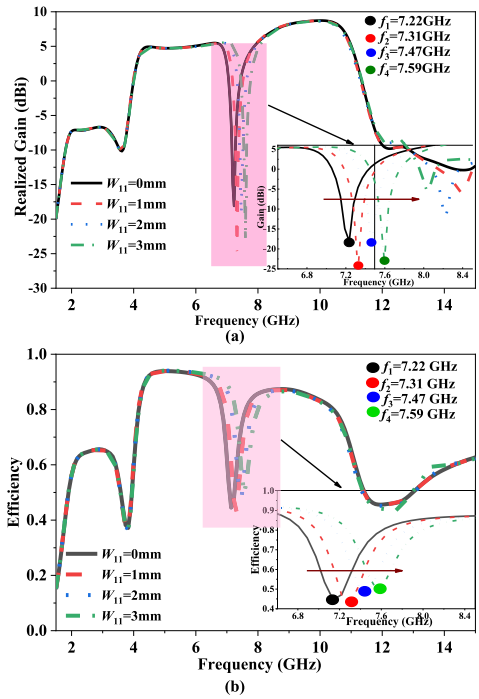

Fig. 15. Effect of the parameter W_{11} on the notched band, (a) Realized gain, (b) Efficiency.

When the W_{11} is changed from 0 to 3mm, the notched frequency is moved from 7.22 to 7.59 GHz, while the null depth better than -15 dBi is well maintained, which means that the suppression level larger than 23.7 dB can be achieved, and the efficiency can maintain less than 50% at the notch.

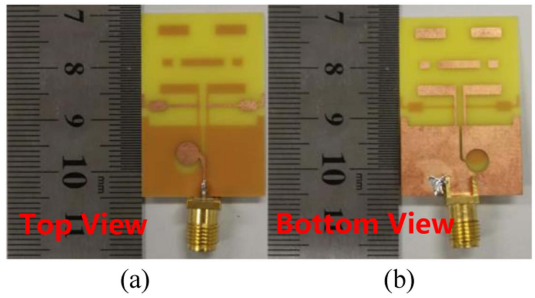

Fig. 16. Photograph of fabricated antenna (a)Top view, (b)Bottom view.

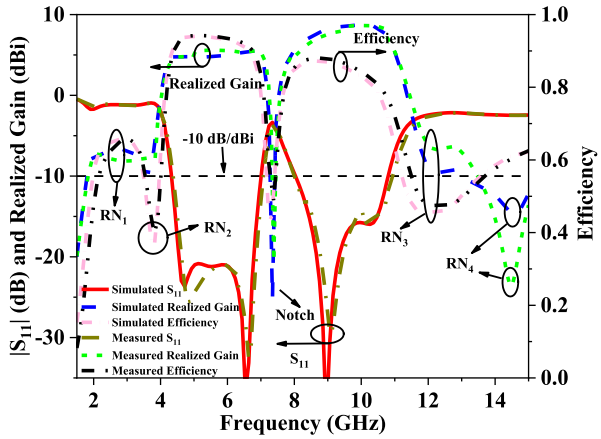

Fig. 17. Measured and simulated results of proposed the filtering band-notched quasi-Yagi antenna.

Therefore, as depicted above, the proposed novel structure can introduce a controllable deep notch band to reject the in-band interferences with the whole performances almost no change, including the S_{11}, realized gain, out-of-band suppressions.

In order to validate the feasibility of the designs, the proposed filtering notched-band quasi-Yagi antenna is designed, fabricated and measured. The dimensions of demonstrated protype are: $L = 35$, $W = 23.5$, $L_1 = 13.5$, $L_2 = 1.95$, $L_3 = 6$, $L_4 = 16.5$, $L_5 = 8.4$, $L_6 = 2.3$, $L_7 = 5$, $L_8 = 6$, $L_9 = 2.6$, $L_{10} = 3.2$, $L_{11} = 0.7$, $L_{12} = 7$, $L_{13} = 3$, $L_{14} = 2$, $W_1 = 0.5$, $W_2 = 0.45$, $W_3 = 1.35$, $W_4 = 1.95$, $W_5 = 1.5$, $W_6 = 1.5$, $W_7 = 5$, $W_8 = 2$, $W_9 = 0.8$, $W_{10} = 0.5$, $W_{11} = 1$, $W_{12} = 0.55$, $W_{13} = 2$, $W_{14} = 0.5$, $r_1 = 2.2$, $r_2 = 1.6$, $r_3 = 2.3$ $r_4 = 0.8$, $D_1 = 2.3$, $D_2 = 4.5$, $D_3 = 1.5$. (Unit: mm). Its photograph is shown in Fig. 16.

Fig. 17 depicts the measured and simulated results of the S parameters and the realized gain. As shown in Fig. 16, the measured results show that the reflection coefficient S_{11} is less than -10 dB from 4.38 to 7.08 GHz and from 8.00 to 10.94 GHz. The notch band is from 7.08 to 8.00 GHz, and the rejection depth of the radiation null is -20.5 dBi at 7.38 GHz with radiation efficiency of only 48%. Besides the maximum and the minimum realized gain of the passband are 8.6 dBi at 10.00 GHz and 4.7 dBi at 4.97 GHz, which is similar with the proposed filtering quasi-Yagi antenna. Fig. 18 is the radiation patterns of the proposed antenna at 6 GHz, the notch frequency and 9 GHz, respectively. The proposed filtering notched-band quasi-Yagi antenna has good endfire characteristics in the passband

TABLE II
COMPARISON OF THE PROPOSED NOTCHED-BAND ANTENNA WITH SOME EXISTING WORKS

Ref.	Design Method	N.B. (GHz)	P.G. (dBi)	N.D. (dBi)	Suppression (dB)	Planar structure	Size (λ_0^2)	Complexity
[24]	Loop radiator + Balun + Multilayer annular disk	2.75-3.3	7.1	-5	12.1	No	0.78×0.78	Complex
[25]	Vivaldi + Resonator	4.9-6.6	8.2	-17	25.2	Yes	0.55×0.44	Simple
[28]	Cross dipole + SRR	2.65-5	9.7	-9	18.7	No	0.64×0.64	Complex
[29]	Full-wavelength dipole array	2.8-3.3	9	-1	10	No	0.86×0.61	Complex
[30]	Cross dipole + Balun + parasitic elements	2.69-3.35	8.1	3.5	4.6	No	0.87×0.87	Complex
[31]	Cross dipole + Balun	2.3-2.51	9	-2	11	No	0.84×0.84	Complex
[32]	Multiobjective evolutionary algorithm + Fragment type etch patterns	5.15-5.85	4	-15	19	Yes	0.3×0.24	Complex
This work	Yagi + Parasitic elements	7.01-8.03	8.7	-25	33.7	Yes	0.51×0.34	Simple

Refs.: References, N.B.: Notch Band, P.G.: Peak Gain, N.D.: Null Depth, Suppression: Peak Gain minus Null Depth

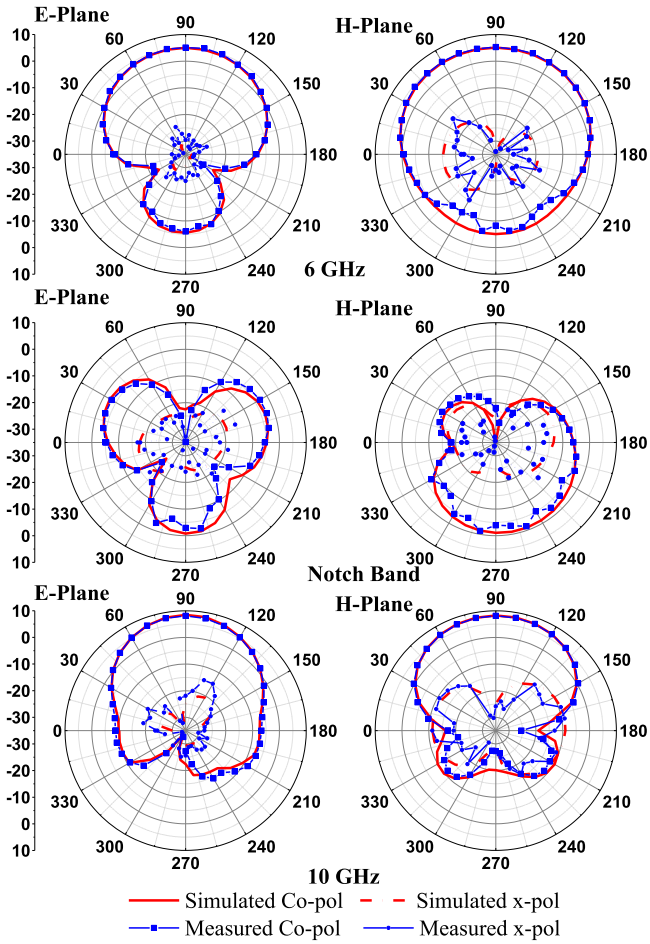

Fig. 18. Radiation patterns at (a) 6 GHz, (b) notch frequency of 7.38 GHz, and (c) 9 GHz.

and good radiation suppression ability in the notch band. The measured cross-polarization levels are less than −15 dB and −10 dB in the E-plane and H-plane across the whole passband, respectively. The little deviation between measured and simulated results can be attributed to SMA connector, unstable dielectric constant, and fabrication error.

In Table II, we list properties of our filtering notched-band antenna and several previously reported antennas with band notch characteristics. It can be found that the proposed prototype has the deepest null rejection, which means it has excellent ability of interference suppression.

IV. CONCLUSION

In this article, a wideband filtering quasi-Yagi antenna using exponential curved branch elements and MST feeding structure is proposed firstly. The MST can not only broaden the bandwidth but also introduce four radiation nulls on the lower and upper stopband inherently. When a pair of exponential curved branch elements are employed, two radiation nulls on the upper stopband are introduced to improve the selectivity of the upper band greatly. Moreover, four parasitic elements are placed around the director to improve the endfire characteristics and the depth of the radiation nulls on the upper stopband, and the bandwidth of 4.46 to 11.31 GHz (∼86.9%), a peak gain of 8.3 dBi and the out-of-band larger than 14 dB are obtained. To meet the requirement of in-band interference suppression, a wideband filtering quasi-Yagi antenna with notched band characteristics is proposed. By adding a pair of L-shaped parasitic elements with SIR characteristics on the top layer, a notch band with −20.5 dBi at 7.38 GHz is introduced in the passband, which results in in-band interference suppression more than 29.1 dBi. Such excellent suppression ability can effectively suppress potential military or satellite interference signals. To further improve the interference suppression ability, and the frequency of the notch can be easily changed by simply controlling the impedance or the electrical length of the L-shaped parasitic elements. Two prototypes are fabricated and measured, the measured and simulated results agree well, and their excellent performances show that the proposed antennas are good candidate for in-vehicle Wi-Fi 6E, in-vehicle satellite communication, mobile-service applications.

REFERENCES

[1] Z. Wang, S. Liu, and Y. Dong, "Compact wideband pattern reconfigurable antennas inspired by end-fire structure for 5G vehicular communication," *IEEE Trans. Veh. Technol.*, vol. 71, no. 5, pp. 4655–4664, May 2022.
[2] L. Chi, Y. Qi, Z. Weng, W. Yu, and W. Zhuang, "A compact wideband slot-loop directional antenna for marine communication applications," *IEEE Trans. Veh. Technol.*, vol. 68, no. 3, pp. 2401–2412, Mar. 2019.
[3] Z.-P. Zhong et al., "A compact dual-band circularly polarized antenna with wide axial-ratio beamwidth for vehicle GPS satellite navigation application," *IEEE Trans. Veh. Technol.*, vol. 68, no. 9, pp. 8683–8692, Sep. 2019.

[4] G. Liu, Y. M. Pan, and X. Y. Zhang, "Compact filtering patch antenna arrays for marine communications," *IEEE Trans. Veh. Technol.*, vol. 69, no. 10, pp. 11408–11418, Oct. 2020.
[5] H. Ozpinar, S. Aksimsek, and N. T. Tokan, "A novel compact, broadband, high gain millimeter-wave antenna for 5G beam steering applications," *IEEE Trans. Veh. Technol.*, vol. 69, no. 3, pp. 2389–2397, Mar. 2020, doi: 10.1109/TVT.2020.2966009.
[6] W. Wu, K.-D. Xu, Q. Chen, T. Tanaka, M. Kozai, and H. Minami, "A wideband reflectarray based on single-layer magneto-electric dipole elements with 1-bit switching mode," *IEEE Trans. Antennas Propag.*, vol. 70, no. 12, pp. 12346–12351, Dec. 2022.
[7] S. Ji, Y. Dong, and Y. Fan, "Bandpass filter prototype inspired filtering patch antenna/array," *IEEE Trans. Antennas Propag.*, vol. 70, no. 5, pp. 3297–3307, May 2022.
[8] K.-R. Xiang, F.-C. Chen, Q. Tan, and Q.-X. Chu, "High-selectivity filtering patch antennas based on MultiPath coupling structures," *IEEE Trans. Microw. Theory Techn.*, vol. 69, no. 4, pp. 2201–2210, Apr. 2021.
[9] S. Kingsly et al., "Multiband reconfigurable filtering monopole antenna for cognitive radio applications," *IEEE Antennas Wireless Propag. Lett.*, vol. 17, no. 8, pp. 1416–1420, Aug. 2018.
[10] J. Deng, S. Hou, L. Zhao, and L. Guo, "Wideband-to-narrowband tunable monopole antenna with integrated bandpass filters for UWB/WLAN applications," *IEEE Antennas Wireless Propag. Lett.*, vol. 16, pp. 2734–2737, 2017, doi: 10.1109/LAWP.2017.2743258.
[11] P. F. Hu, Y. M. Pan, X. Y. Zhang, and B. J. Hu, "A compact quasi-isotropic dielectric resonator antenna with filtering response," *IEEE Trans. Antennas Propag.*, vol. 67, no. 2, pp. 1294–1299, Feb. 2019.
[12] P. F. Hu, Y. M. Pan, X. Y. Zhang, and S. Y. Zheng, "Broadband filtering dielectric resonator antenna with wide stopband," *IEEE Trans. Antennas Propag.*, vol. 65, no. 4, pp. 2079–2084, Apr. 2017.
[13] J. Wu, Z. Zhao, Z. Nie, and Q. H. Liu, "A broadband unidirectional antenna based on closely spaced loading method," *IEEE Trans. Antennas Propag.*, vol. 61, no. 1, pp. 109–116, Jan. 2013.
[14] J. Wu, Z. Zhao, Z. Nie, and Q.-H. Liu, "A printed unidirectional antenna with improved upper band-edge selectivity using a parasitic loop," *IEEE Trans. Antennas Propag.*, vol. 63, no. 4, pp. 1832–1837, Apr. 2015.
[15] W. Zhou, J. Liu, and Y. Long, "A broadband and high-gain planar complementary Yagi array antenna with circular polarization," *IEEE Trans. Antennas Propag.*, vol. 65, no. 3, pp. 1446–1451, Mar. 2017.
[16] J. Shi et al., "A compact differential filtering quasi-Yagi antenna with high frequency selectivity and low cross-polarization levels," *IEEE Antennas Wireless Propag. Lett.*, vol. 14, pp. 1573–1576, 2015.
[17] J. Zang, X. Wang, A. Alvarez-Melcon, and J. S. Gomez-Diaz, "Nonreciprocal Yagi–Uda filtering Antennas," *IEEE Antennas Wireless Propag. Lett.*, vol. 18, no. 12, pp. 2661–2665, Dec. 2019.
[18] F. Wei, X.-B. Zhao, and X. W. Shi, "A balanced filtering quasi-Yagi antenna with low cross-polarization levels and high common-mode suppression," *IEEE Access*, vol. 7, pp. 100113–100119, 2019.
[19] K. Xu, H. Xu, and Y. Liu, "Low-profile filtering end-fire antenna integrated with compact bandstop filtering element for high selectivity," *IEEE Access*, vol. 7, pp. 8398–8403, 2019.
[20] G. Liu, Y. M. Pan, T. L. Wu, and P. F. Hu, "A compact planar quasi-Yagi antenna with bandpass filtering response," *IEEE Access*, vol. 7, pp. 67856–67862, 2019.
[21] S. Wang et al., "A planar absorptive-branch-loaded quasi-Yagi antenna with filtering capability and flat gain," *IEEE Antennas Wireless Propag. Lett.*, vol. 20, no. 9, pp. 1626–1630, Sep. 2021.
[22] Y.-H. Ke, L.-L. Yang, Y.-Y. Zhu, J. Wang, and J.-X. Chen, "Filtering quasi-Yagi strip-loaded DRR antenna with enhanced gain and selectivity by metamaterial," *IEEE Access*, vol. 9, pp. 31755–31761, 2021.
[23] H. U. Bong, M. Jeong, N. Hussain, S. Y. Rhee, S. K. Gil, and N. Kim, "Design of an UWB antenna with two slits for 5G/WLAN-notched bands," *Microw. Opt. Technol. Lett.*, vol. 61, no. 5, pp. 1295–1300, 2019.
[24] Z. Li, J. Han, Y. Mu, X. Gao, and L. Li, "Dual-band Dual-polarized base station antenna with a notch band for 2/3/4/5G communication systems," *IEEE Antennas Wireless Propag. Lett.*, vol. 19, no. 12, pp. 2462–2466, Dec. 2020.
[25] Y. Xu, J. Wang, L. Ge, X. Wang, and W. Wu, "Design of a notched-band Vivaldi Antenna with high selectivity," *IEEE Antennas Wireless Propag. Lett.*, vol. 17, no. 1, pp. 62–65, Jan. 2018.
[26] S. u. Rehman and M. A. S. Alkanhal, "Design and system characterization of ultra-wideband antennas with multiple band-rejection," *IEEE Access*, vol. 5, pp. 17988–17996, 2017.
[27] C. Chen, "A compact wideband endfire filtering antenna inspired by a uniplanar microstrip antenna," *IEEE Antennas Wireless Propag. Lett.*, vol. 21, no. 4, pp. 853–857, Apr. 2022.
[28] Y. Zhang, Y. Zhang, D. Li, K. Liu, and Y. Fan, "Dual-polarized band-notched antenna without extra circuit for 2.4/5 GHz WLAN applications," *IEEE Access*, vol. 7, pp. 84890–84896, 2019.
[29] C. Ding, H.-H. Sun, H. Zhu, and Y. Jay Guo, "Achieving wider bandwidth with full-wavelength dipoles for 5G base stations," *IEEE Trans. Antennas Propag.*, vol. 68, no. 2, pp. 1119–1127, Feb. 2020.
[30] S. Fu, Z. Cao, X. Quan, and C. Xu, "A broadband dual-polarized notched-band antenna for 2/3/4/5G base station," *IEEE Antennas Wireless Propag. Lett.*, vol. 19, no. 1, pp. 69–73, Jan. 2020.
[31] H. Huang, Y. Liu, and S. Gong, "A broadband dual-polarized base station antenna with anti-interference capability," *IEEE Antennas Wireless Propag. Lett.*, vol. 16, pp. 613–616, 2017.
[32] Y. Du, X. Wu, J. Sidén, and G. Wang, "Design of sharp roll-off band notch with fragment-type pattern etched on UWB antenna," *IEEE Antennas Wireless Propag. Lett.*, vol. 17, no. 12, pp. 2404–2408, Dec. 2018.

Daotong Li (Senior Member, IEEE) received the Ph.D. degree in electromagnetic field and microwave technology from the University of Electronic Science and Technology of China (UESTC), Chengdu, China, in 2016.

Since 2015, he has been a Visiting Researcher with the Department of Electrical and Computer Engineering, University of Illinois at Urbana–Champaign, Urbana, IL, USA, with financial support from the China Scholarship Council. In 2017, he joined the Center of Communication and Tracking Telemetry Command, Chongqing University, as an Assistant Professor. In 2019, he was promoted to Associate Professor. He has authored or coauthored more than 100 peer-reviewed journal and conference papers. He is currently with the Center of Communication and Tracking Telemetry Command, Chongqing University, Chongqing, China.

His research interests include RF, microwave and millimeter-wave technology and applications, microwave power transmission (MPT), antennas, devices, circuits and systems, and passive and active (sub-) millimeter-wave imaging and radiometer. Dr. Li was the recipient of the UESTC Outstanding Graduate awards by the Sichuan province and UESTC in 2016, the National Graduate Student Scholarship from the Ministry of Education, China, and "Tang Lixin" Scholarship. He is also a Reviewer for several IEEE and IET journals, and many international conferences as a TPC Member, a Session Organizer, and the Session Chair. Since November 2021, he has been the recipient of the Fellowship from the Japan Society for the Promotion of Science (JSPS) and has been the JSPS Fellow with the Department of Communications Engineering, Graduate School of Engineering, Tohoku University.

Chen Yang received the B.S. degree in communication engineering in 2021 from Chongqing University, Chongqing, China, where he is currently working toward the M.S. degree in electronic information. His research interests include filtering antennas and filters.

Ying Liu received the B.E. degree in communications engineering from the Qingdao University of Science and Technology, Qingdao, Shandong, China, in 2012, and the M.S. degree in communication and information system from the Chongqing University, Chongqing, China, in 2015. She is currently with the School of Microelectronics and Communication Engineering, Chongqing University.

Her research interests include microwave and optical image processing, and microwave photonics.

Lisheng Yang received the B.S. degree in radio technology, and the M.S. and Ph.D. degrees in circuit and systems from Chongqing University, Chongqing, China, in 1992, 2004, and 2006, respectively.

He was a Researcher and Doctoral Supervisor with the Institute of Aerocraft Tracking, Microelectronics and Communications Engineering, Chongqing University. From 2004 to 2005, he was the Key Innovation Platform of the National "985 Project" and responsible for the research on formation flight satellite measurement and control system of the China Academy of Aerospace Science and Industry Information Technology. Since 2005, he has been the backbone of the CNGI Project of the National Development and Reform Commission, responsible for the research and development of the cngi-ap multi-user smart antenna system. He was supported by the New Century Excellent Talents Support Program of the Ministry of Education, in 2007. His research interests include 5G, software radio, wireless sensor networks, and metamaterials. Dr. Yang was the recipient of the Second Prize of the National Science and Technology Progress Award, in 2004, and the Third Winner.

Qiang Chen (Senior Member, IEEE) received the B.E. degree from Xidian University, Xi'an, China, in 1986, the M.E. and D.E. degrees from Tohoku University, Sendai, Japan, in 1991 and 1994, respectively. He is currently the Chair Professor with Electromagnetic Engineering Laboratory, Department of Communications Engineering, Faculty of Engineering, Tohoku University. His research interests include antennas, microwave and millimeter wave, electromagnetic measurement, and computational electromagnetics.

From 2012 to 2014, he was also the Chair of IEICE Technical Committee on Photonics-applied Electromagnetic Measurement, Chair of IEICE Technical Committee on Wireless Power Transfer from 2016 to 2018, Chair of IEEE Antennas and Propagation Society Tokyo Chapter from 2017 to 2018, Chair of IEICE Technical Committee on Antennas and Propagation from 2019 to 2021. He was the recipient of the Best Paper Award and Zenichi Kiyasu Award from the Institute of Electronics, Information and Communication Engineers (IEICE). Dr. Chen is the Fellow of Institute of Electronics, Information, and Communication Engineers (IEICE).